

Contents

1	Introduction	2
2	The convection–diffusion equations	3
2.1	Reynolds transport theorem	3
2.2	Continuity equation	3
2.3	Momentum equation	3
2.4	Energy equation	3
2.5	Species equation	3
2.6	Convection–diffusion equations	3
3	Numerical study	4
3.1	Assumptions	4
3.2	Spatial discretization	4
3.3	Time discretization	5
3.4	Discretization of the continuity equation	5
3.5	Discretization of the general convection–diffusion equation	6
3.6	Evaluation of the convective terms	8
3.6.1	Upwind–Difference Scheme (UDS)	8
3.6.2	Central–Difference Scheme (CDS)	9
3.6.3	Quadratic Upwind Interpolation for Convective Kinematics (QUICK)	10

1 Introduction

2 The convection–diffusion equations

2.1 Reynolds transport theorem

$$\frac{d}{dt} \int_{V(t)} F(\mathbf{x}, t) d\mathbf{x} = \int_{V(t)} \frac{\partial F}{\partial t} d\mathbf{x} + \int_{A(t)} F(\mathbf{x}, t) \mathbf{b} \cdot \mathbf{n} dS \quad (2.1)$$

2.2 Continuity equation

$$\frac{\partial \rho}{\partial t} + \nabla \cdot (\rho \mathbf{v}) = 0 \quad (2.2)$$

2.3 Momentum equation

$$\frac{\partial(\rho \mathbf{v})}{\partial t} + \nabla \cdot (\rho \mathbf{v} \otimes \mathbf{v}) = \nabla \cdot (\mu \nabla \mathbf{v}) + \{ \nabla \cdot (\tau - \mu \nabla \mathbf{v}) - \nabla p + \rho \mathbf{g} \} \quad (2.3)$$

2.4 Energy equation

$$\frac{\partial(\rho T)}{\partial t} + \nabla \cdot (\rho \mathbf{v} T) = \nabla \cdot \left(\frac{\lambda}{c_v} \nabla T \right) + \left\{ \frac{\tau \circ \nabla \mathbf{v} - \nabla \cdot \dot{\mathbf{q}}^R - p \nabla \cdot \mathbf{v}}{c_v} \right\} \quad (2.4)$$

2.5 Species equation

$$\frac{\partial(\rho Y_k)}{\partial t} + \nabla \cdot (\rho \mathbf{v} Y_k) = \nabla \cdot (\rho D_{km} \nabla Y_k) + \{ \dot{\omega}_k \} \quad (2.5)$$

2.6 Convection–diffusion equations

3 Numerical study

3.1 Assumptions

In order to solve the convection–diffusion equations numerically, we must make some assumptions which will simplify our study.

1. The location where the problem takes place is a closed connected set K contained in a bounded open connected set $\Omega \subset \mathbb{R}^m$, where $m = 1, 2, 3$ depends on the dimension of the problem. Both K and Ω are \mathcal{C}^1 or Lipschitz domains, allowing us to use vector calculus theorems.
2. The problem lasts for finite time, starting at time $t = 0$ and ending at time $t = t_{\max}$. Therefore the time interval is $I = (0, t_{\max}) \subset \mathbb{R}$.
3. The closed connected set K can be expressed as the union of finitely many closed sets $\mathcal{V}_1, \dots, \mathcal{V}_r$, that is, $K = \mathcal{V}_1 \cup \dots \cup \mathcal{V}_r$. Moreover, these sets

The control volume centered at node P will be denoted by \mathcal{V}_P . Its boundary, known as the control surface, will be expressed as $\mathcal{S}_P = \partial\mathcal{V}_P$. The volume \mathcal{V}_P occupies in \mathbb{R}^m

3.2 Spatial discretization

The type of problems addressed in this project occur in a bounded domain $\Omega \subset \mathbb{R}^m$ with $1 \leq m \leq 3$ depending on the case. In order to solve the problem numerically, a control–volume formulation is followed. This methodology discretizes the domain into nonoverlapping control volumes along with a grid of points named discretization nodes. The resulting discretized domain is named mesh or numerical grid [1].

There exist several types of grids according to the shape of control volumes and the ammount of subdivisions the domain has been partitioned into [2]:

- Structured (regular) grid:
- Block–structured grid:
- Unstructured grid:

Hereinafter, a structured regular grid approach will be followed. This formulation allows for two manners to discretize the domain, namely, cell–centered and node–centered discretizations. The former places discretization nodes over the domain and generates a control–volume centered on each node. The latter first generates the control–volumes and then places a node at the center of each one.



Figure 3.1. A figure with two subfigures

3.3 Time discretization

3.4 Discretization of the continuity equation

As seen before, the continuity equation in differential form is

$$\frac{\partial \rho}{\partial t} + \nabla \cdot (\rho \mathbf{v}) = 0 \quad (\mathbf{x}, t) \in \Omega \times I \quad (3.1)$$

Since the above relation is true on $\Omega \times I$, fixing one time $t \in I$ and integrating over a control volume $\mathcal{V}_P \subset \Omega$ yields

$$\int_{\mathcal{V}_P} \frac{\partial \rho}{\partial t} d\mathbf{x} + \int_{\mathcal{V}_P} \nabla \cdot (\rho \mathbf{v}) d\mathbf{x} = 0 \quad (3.2)$$

Let $\mathcal{S}_P = \partial \mathcal{V}_P$ be the control surface, i.e. the boundary of the control volume. Then applying the divergence theorem on the second term of equation (3.2)

$$\int_{\mathcal{V}_P} \frac{\partial \rho}{\partial t} d\mathbf{x} + \int_{\mathcal{S}_P} \rho \mathbf{v} \cdot \mathbf{n} dS = 0 \quad (3.3)$$

With the aim of simplifying the first term of (3.3), the average density of the control volume is defined as

$$\bar{\rho}_P = \frac{1}{V_P} \int_{\mathcal{V}_P} \rho d\mathbf{x} \quad (3.4)$$

Introducing this relation in equation (3.3) gives

$$\frac{d\bar{\rho}_P}{dt} V_P + \int_{\mathcal{S}_P} \rho \mathbf{v} \cdot \mathbf{n} dS = 0 \quad (3.5)$$

The mass flow term can be further simplified if a cartesian mesh is being used. In case of a 2D-mesh, the control surface can be partitioned into four different faces, namely, the east, west, north and south faces. In this context the control surface is $\mathcal{S}_P = \mathcal{S}_{Pe} \cup \mathcal{S}_{Pw} \cup \mathcal{S}_{Pn} \cup \mathcal{S}_{Ps}$ and the mass flow term may be expressed as

$$\int_{\mathcal{S}_P} \rho \mathbf{v} \cdot \mathbf{n} dS = \sum_i \int_{\mathcal{S}_{Pi}} \rho \mathbf{v} \cdot \mathbf{n} dS = \dot{m}_e + \dot{m}_w + \dot{m}_n + \dot{m}_s \quad (3.6)$$

If on the other hand a 3D-mesh is being used, the contributions of top and bottom faces must be considered. The control surface is the union $\mathcal{S}_P = \mathcal{S}_{Pe} \cup \mathcal{S}_{Pw} \cup \mathcal{S}_{Pn} \cup \mathcal{S}_{Ps} \cup \mathcal{S}_{Pt} \cup \mathcal{S}_{Pb}$, and therefore the mass flow incorporates two new terms

$$\int_{\mathcal{S}_P} \rho \mathbf{v} \cdot \mathbf{n} dS = \sum_i \int_{\mathcal{S}_{Pi}} \rho \mathbf{v} \cdot \mathbf{n} dS = \dot{m}_e + \dot{m}_w + \dot{m}_n + \dot{m}_s + \dot{m}_t + \dot{m}_b \quad (3.7)$$

This allows writing equation (3.5) in the following way

$$\frac{d\bar{\rho}_P}{dt} V_P + \sum_i \dot{m}_i = 0 \quad (3.8)$$

The average density of the control volume is roughly the density at the discretization node, that is, $\bar{\rho}_P \approx \rho_P$. Integrating (3.8) over the time interval $[t^n, t^{n+1}]$ gives

$$V_P \int_{t^n}^{t^{n+1}} \frac{d\bar{\rho}_P}{dt} dt + \int_{t^n}^{t^{n+1}} \sum_i \dot{m}_i dt = 0 \quad (3.9)$$

The first term of (3.9) has a straightforward simplification applying a corollary of the fundamental theorem of calculus. Regarding the second term, numerical integration is applied,

$$(\rho_P^{n+1} - \rho_P^n) V_P + \left(\beta \sum_i \dot{m}_i^{n+1} + (1 - \beta) \sum_i \dot{m}_i^n \right) (t^{n+1} - t^n) = 0 \quad (3.10)$$

where $\beta \in \{0, \frac{1}{2}, 1\}$ depends on the chosen integration scheme. For the sake of simplicity, superindex $n + 1$ shall be dropped and the time instant n will be denoted by the superindex 0. Assuming a uniform time step Δt , the resulting discretized continuity equation is

$$\frac{\rho_P - \rho_P^0}{\Delta t} V_P + \beta \sum_i \dot{m}_i + (1 - \beta) \sum_i \dot{m}_i^0 = 0 \quad (3.11)$$

3.5 Discretization of the general convection–diffusion equation

The generalized convection–diffusion for a real valued function $\phi: \Omega \times I \subset \mathbb{R}^m \times \mathbb{R} \rightarrow \mathbb{R}$ is

$$\frac{\partial(\rho\phi)}{\partial t} + \nabla \cdot (\rho \mathbf{v} \phi) = \nabla \cdot (\Gamma_\phi \nabla \phi) + \dot{s}_\phi, \quad (\mathbf{x}, t) \in \Omega \times I \quad (3.12)$$

whereas for a vector valued function $\phi = (\phi_1, \dots, \phi_m): \Omega \times I \subset \mathbb{R}^m \times \mathbb{R} \rightarrow \mathbb{R}^m$ it is written as

$$\frac{\partial(\rho\phi)}{\partial t} + \nabla \cdot (\rho \mathbf{v} \otimes \phi) = \nabla \cdot (\Gamma_\phi \nabla \phi) + \dot{s}_\phi, \quad (\mathbf{x}, t) \in \Omega \times I \quad (3.13)$$

Since the generalized convection–diffusion equation for a vector valued function actually comprises m equations, one for each component function, only the discretization for a real valued function will be studied.

Integrating over $\mathcal{V}_P \times [t^n, t^{n+1}] \subset \Omega \times I$ and using Fubini's theorem

$$\begin{aligned} \int_{t^n}^{t^{n+1}} \int_{\mathcal{V}_P} \frac{\partial(\rho\phi)}{\partial t} d\mathbf{x} dt + \int_{t^n}^{t^{n+1}} \int_{\mathcal{V}_P} \nabla \cdot (\rho \mathbf{v} \phi) d\mathbf{x} dt &= \\ &= \int_{t^n}^{t^{n+1}} \int_{\mathcal{V}_P} \nabla \cdot (\Gamma_\phi \nabla \phi) d\mathbf{x} dt + \int_{t^n}^{t^{n+1}} \int_{\mathcal{V}_P} \dot{s}_\phi d\mathbf{x} dt \end{aligned} \quad (3.14)$$

Each term is developed separately. The simplification of the first term is analogous to that of the continuity equation. The average value of $\rho\phi$ in \mathcal{V}_P at time t is defined by

$$(\rho\phi)_P = \frac{1}{V_P} \int_{\mathcal{V}_P} \rho\phi d\mathbf{x} \quad (3.15)$$

then

$$\int_{t^n}^{t^{n+1}} \int_{\mathcal{V}_P} \frac{\partial(\rho\phi)}{\partial t} d\mathbf{x} dt = \int_{t^n}^{t^{n+1}} \frac{d}{dt} \int_{\mathcal{V}_P} \rho\phi d\mathbf{x} dt = \int_{t^n}^{t^{n+1}} \frac{d(\rho\phi)_P}{dt} V_P dt = \left\{ (\rho\phi)_P - (\rho\phi)_P^0 \right\} V_P \quad (3.16)$$

Divergence theorem must be applied to simplify the convective contribution,

$$\int_{t^n}^{t^{n+1}} \int_{\mathcal{V}_P} \nabla \cdot (\rho \mathbf{v} \phi) d\mathbf{x} dt = \int_{t^n}^{t^{n+1}} \int_{S_P} \rho \phi \mathbf{v} \cdot \mathbf{n} dS dt = \int_{t^n}^{t^{n+1}} \sum_i \int_{S_{Pi}} \rho \phi \mathbf{v} \cdot \mathbf{n} dS dt \quad (3.17)$$

The value that ϕ takes on \mathcal{S}_{P_i} can be approximated by its value at a representative point, that is to say, $\phi \approx \phi_i$. Therefore,

$$\begin{aligned} \int_{t^n}^{t^{n+1}} \sum_i \int_{\mathcal{S}_i} \rho \phi \mathbf{v} \cdot \mathbf{n} dS dt &\approx \int_{t^n}^{t^{n+1}} \sum_i \int_{\mathcal{S}_i} \rho \phi_i \mathbf{v} \cdot \mathbf{n} dS dt = \int_{t^n}^{t^{n+1}} \sum_i \dot{m}_i \phi_i dt = \\ &= \left\{ \beta \sum_i \dot{m}_i \phi_i + (1 - \beta) \sum_i \dot{m}_i^0 \phi_i^0 \right\} \Delta t \quad (3.18) \end{aligned}$$

For the third term,

$$\int_{t^n}^{t^{n+1}} \int_{\mathcal{V}_P} \nabla \cdot (\Gamma_\phi \nabla \phi) d\mathbf{x} dt = \int_{t^n}^{t^{n+1}} \int_{\mathcal{S}_P} \Gamma_\phi \nabla \phi \cdot \mathbf{n} dS dt = \int_{t^n}^{t^{n+1}} \sum_i \int_{\mathcal{S}_{P_i}} \Gamma_\phi \nabla \phi \cdot \mathbf{n} dS dt \quad (3.19)$$

Since a cartesian mesh is being used, the outer normal vector to the face \mathcal{S}_{P_i} is constant and points in the direction of some coordinate axis. Hence the dot product $\nabla \phi \cdot \mathbf{n}$ in the face \mathcal{S}_{P_i} equals the partial derivative with respect to x_i times ± 1 , depending on the direction of \mathbf{n} . For east, north and top faces the sign is positive, whilst for west, south and bottom faces the sign is negative. Again, the values Γ_ϕ and of the partial derivative at the face \mathcal{S}_i will be approximated by the value at a representative point of the face and by a finite centered difference, respectively. In order to simplify the notation, the subindex ϕ in the diffusion coefficient Γ_ϕ will be dropped. As a result, for a 2D-mesh the discretization is the following,

$$\begin{aligned} \int_{t^n}^{t^{n+1}} \sum_i \int_{\mathcal{S}_{P_i}} \Gamma_\phi \nabla \phi \cdot \mathbf{n} dS dt &\approx \\ &\approx \int_{t^n}^{t^{n+1}} \left\{ \Gamma_e \frac{\phi_E - \phi_P}{d_{PE}} S_e - \Gamma_w \frac{\phi_P - \phi_W}{d_{PW}} S_w + \Gamma_n \frac{\phi_N - \phi_P}{d_{PN}} S_n - \Gamma_s \frac{\phi_P - \phi_S}{d_{PS}} S_s \right\} dt \approx \\ &\approx \beta \left\{ \Gamma_e \frac{\phi_E - \phi_P}{d_{PE}} S_e - \Gamma_w \frac{\phi_P - \phi_W}{d_{PW}} S_w + \Gamma_n \frac{\phi_N - \phi_P}{d_{PN}} S_n - \Gamma_s \frac{\phi_P - \phi_S}{d_{PS}} S_s \right\} \Delta t + \\ &+ (1 - \beta) \left\{ \Gamma_e^0 \frac{\phi_E^0 - \phi_P^0}{d_{PE}} S_e - \Gamma_w^0 \frac{\phi_P^0 - \phi_W^0}{d_{PW}} S_w + \Gamma_n^0 \frac{\phi_N^0 - \phi_P^0}{d_{PN}} S_n - \Gamma_s^0 \frac{\phi_P^0 - \phi_S^0}{d_{PS}} S_s \right\} \Delta t \quad (3.20) \end{aligned}$$

In case of a 3D-mesh, the contributions of top and bottom faces must be accounted for.

In order to discretize the fourth term, the mean value of the source in \mathcal{V}_P at an instant t is defined as follows

$$\bar{s}_\phi = \frac{1}{V_P} \int_{\mathcal{V}_P} \dot{s}_\phi d\mathbf{x} \quad (3.21)$$

If the value of s_ϕ is known, the relation $\bar{s}_\phi = \dot{s}_\phi$ is true. Indeed,

$$\dot{\bar{s}}_\phi = \frac{d}{dt} \bar{s}_\phi = \frac{1}{V_P} \frac{d}{dt} \int_{\mathcal{V}_P} s_\phi d\mathbf{x} = \frac{1}{V_P} \int_{\mathcal{V}_P} \dot{s}_\phi d\mathbf{x} = \bar{s}_\phi \quad (3.22)$$

In most cases, the dependence of $\dot{\bar{s}}_\phi$ on ϕ is complicated. Since the equations obtained until now are linear, the relation between the source term and the variable would ideally be linear. This linearity is imposed as follows

$$\dot{\bar{s}}_\phi = S_C^\phi + S_P^\phi \phi_P \quad (3.23)$$

where the values of S_C^ϕ and S_P^ϕ may vary with ϕ [1]. Making use of these relations, the source term integral is discretized as

$$\int_{t^n}^{t^{n+1}} \int_{\mathcal{V}_P} \dot{s}_\phi d\mathbf{x} dt = \int_{t^n}^{t^{n+1}} \dot{\bar{s}}_{\phi P} V_P \Delta t = (S_C^\phi + S_P^\phi \phi_P) V_P \Delta t \quad (3.24)$$

Finally, the discretization of the generalized convection–diffusion equation is

$$\begin{aligned}
& \frac{(\rho\phi)_P - (\rho\phi)_P^0}{\Delta t} V_P + \\
& + \beta (\dot{m}_e \phi_e - \dot{m}_w \phi_w + \dot{m}_n \phi_n - \dot{m}_s \phi_s) + (1 - \beta) (\dot{m}_e^0 \phi_e^0 - \dot{m}_w^0 \phi_w^0 + \dot{m}_n^0 \phi_n^0 - \dot{m}_s^0 \phi_s^0) = \\
& = \beta \left\{ \Gamma_e \frac{\phi_E - \phi_P}{d_{PE}} S_e - \Gamma_w \frac{\phi_P - \phi_W}{d_{PW}} S_w + \Gamma_n \frac{\phi_N - \phi_P}{d_{PN}} S_n - \Gamma_s \frac{\phi_P - \phi_S}{d_{PS}} S_s \right\} + \\
& + (1 - \beta) \left\{ \Gamma_e^0 \frac{\phi_E^0 - \phi_P^0}{d_{PE}} S_e - \Gamma_w^0 \frac{\phi_P^0 - \phi_W^0}{d_{PW}} S_w + \Gamma_n^0 \frac{\phi_N^0 - \phi_P^0}{d_{PN}} S_n - \Gamma_s^0 \frac{\phi_P^0 - \phi_S^0}{d_{PS}} S_s \right\} + \\
& + (S_C^\phi + S_P^\phi \phi_P) V_P
\end{aligned} \tag{3.25}$$

3.6 Evaluation of the convective terms

As seen before, the discretization of the generalized convection–diffusion equations requires the values of certain variables at points different from the nodes. In this section several methods to compute ϕ at faces are given. The values of ρ and Γ will be assumed to be known at the nodal points. East face will be taken as reference for simplicity. The generalization to the remaining faces is straightforward.

3.6.1 Upwind–Difference Scheme (UDS)

Incompressible flows and gases at low Mach number are more influenced by upstream conditions than downstream conditions. Let $(\mathbf{v} \cdot \mathbf{n})_e$ denote the value of the dot product $\mathbf{v} \cdot \mathbf{n}$ at east face \mathcal{S}_{Pe} . If $(\mathbf{v} \cdot \mathbf{n})_e > 0$, fluid flows from node P to node E , hence P is the upstream node and E is the downstream node. Conversely, if $(\mathbf{v} \cdot \mathbf{n})_e < 0$, nodes interchange their roles as fluid flows from node E to node P . This situation is pictured in figures 3.2 and 3.3.

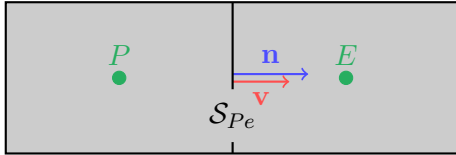


Figure 3.2. Since $(\mathbf{v} \cdot \mathbf{n})_e > 0$ fluid flows from node P (upstream node) to node E (downstream node).

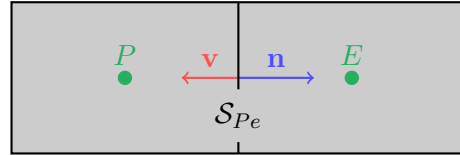


Figure 3.3. Since $(\mathbf{v} \cdot \mathbf{n})_e < 0$ fluid flows from node E (upstream node) to node P (downstream node).

If $(\mathbf{v} \cdot \mathbf{n})_e = 0$, it implies \mathbf{v}_e lies in the orthogonal subspace to the vector space generated by \mathbf{n} . As a result, given the approximations taken, there is no fluid flow through face \mathcal{S}_{Pe} .

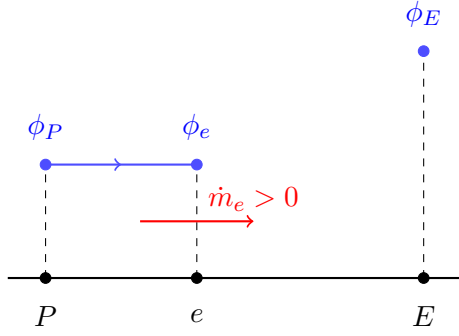
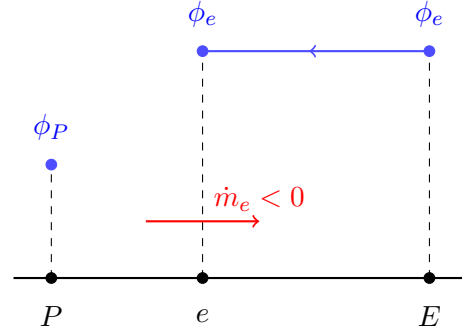
The Upwind–Difference Scheme assigns ϕ_e the value of ϕ at the upstream node, that is,

$$\phi_e^{\text{UDS}} = \begin{cases} \phi_P & \text{if } (\mathbf{v} \cdot \mathbf{n})_e > 0 \\ \phi_E & \text{if } (\mathbf{v} \cdot \mathbf{n})_e < 0 \end{cases} \tag{3.26}$$

This can be expressed in a more compact form as follows

$$\dot{m}_e (\phi_e^{\text{UDS}} - \phi_P) = \frac{\dot{m}_e - |\dot{m}_e|}{2} (\phi_E - \phi_P) \tag{3.27}$$

since the approximation to compute \dot{m}_e is related to $(\mathbf{v} \cdot \mathbf{n})_e$ through the relation $\dot{m}_e = (\mathbf{v} \cdot \mathbf{n})_e S_{Pe}$. The scheme is shown in figures 3.4 and 3.5.

**Figure 3.4.** UDS when $(\mathbf{v} \cdot \mathbf{n})_e > 0$.**Figure 3.5.** UDS when $(\mathbf{v} \cdot \mathbf{n})_e < 0$.

UDS is a stable scheme, however it suffers from numerical diffusion. Indeed, assuming the upstream node is P and expanding ϕ about the point x_P in its Taylor expansion up to 2nd degree,

$$\phi_e = \phi_P + \left(\frac{\partial \phi}{\partial x} \right)_P d_{Pe} + \left(\frac{\partial^2 \phi}{\partial x^2} \right)_{\xi_1} \frac{d_{Pe}^2}{2} \quad (3.28)$$

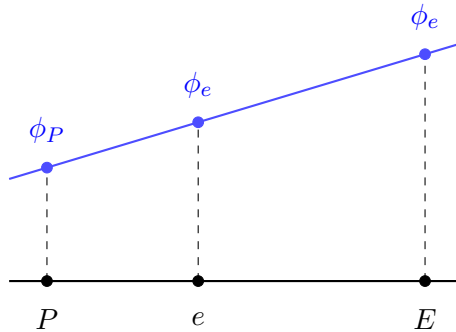
it is apparent that UDS retains the first term on the left-hand side of (3.28). As a consequence, the highest order term of the error is $(\partial_x \phi)_P d_{Pe}$, which is proportional to the distance between P and the face \mathcal{S}_{Pe} . This term resembles to a diffusion flux given, for instance, by Fourier's or Fick's laws of diffusion. The same result is obtained when E is the upstream node,

$$\phi_e = \phi_E - \left(\frac{\partial \phi}{\partial x} \right)_E d_{Ee} + \left(\frac{\partial^2 \phi}{\partial x^2} \right)_{\xi_2} \frac{d_{Ee}^2}{2} \quad (3.29)$$

whence it can be deduced that the error is bounded by $\max\{ |(\partial_x \phi)_E d_{Pe}|, |(\partial_x \phi)_E d_{Ee}| \}$. The numerical diffusion issue is magnified in multidimensional problems, where peaks of rapid variation can be obtained, hence very fine grids are required.

3.6.2 Central-Difference Scheme (CDS)

CDS assumes a linear distribution for ϕ as illustrated in figure 3.6,

**Figure 3.6.** Central Difference Scheme (CDS)

Thereby ϕ_e can be obtained interpolating between ϕ_P and ϕ_E ,

$$\phi_e - \phi_P = f_e (\phi_E - \phi_P), \quad f_e = \frac{d_{Pe}}{d_{PE}} \quad (3.30)$$

This yields a 2nd order approximation for ϕ_e if $d_{Pe} = d_{Ee}$. Indeed, applying Taylor's theorem about the point x_e and using Lagrange's remainder,

$$\phi_P = \phi_e - \left(\frac{\partial \phi}{\partial x} \right)_e d_{Pe} + \frac{1}{2} \left(\frac{\partial^2 \phi}{\partial x^2} \right)_e d_{Pe}^2 + \frac{1}{6} \left(\frac{\partial^3 \phi}{\partial x^3} \right)_{\xi_1} d_{Pe}^3 \quad (3.31)$$

where ξ_1 is some point lying in the convex combination of (x_P, y_P) and $(x_E, y_E) = (x_E, y_P)$, that is, a point contained in the set $\{(\lambda x_E + (1 - \lambda)x_P, y_P) \mid \lambda \in (0, 1)\}$. On the other hand, the 2nd order approximation of the derivative $(\partial_x \phi)_e$ is given by

$$\left(\frac{\partial \phi}{\partial x} \right)_e = \frac{\phi_E - \phi_P}{d_{PE}} - \left(\frac{\partial^3 \phi}{\partial x^3} \right)_{\xi_2} \frac{d_{PE}^2}{3!} = \frac{\phi_E - \phi_P}{d_{PE}} - \left(\frac{\partial^3 \phi}{\partial x^3} \right)_{\xi_2} \frac{(d_{Pe} + d_{Ee})^2}{3!} \quad (3.32)$$

where, again, ξ_2 is some point obtained as the convex combination of (x_P, y_P) and (x_E, y_E) . Introducing (3.32) in (3.31) and imposing $d_{Pe} = d_{Ee}$,

$$\phi_e - \phi_P = \frac{d_{Pe}}{d_{PE}}(\phi_E - \phi_P) - \left(\frac{\partial^2 \phi}{\partial x^2} \right)_e \frac{d_{Pe}^2}{2} - \left\{ \left(\frac{\partial^3 \phi}{\partial x^3} \right)_{\xi_1} + 4 \left(\frac{\partial^3 \phi}{\partial x^3} \right)_{\xi_2} \right\} \frac{d_{Pe}^3}{6} \quad (3.33)$$

As CDS retains the first term on the left-hand side of (3.33), the highest order term of the error is $\frac{1}{2}(\partial_x^2 \phi)_e d_{Pe}^2$, proving that CDS provides a 2nd order approximation of ϕ_e when $d_{Pe} = d_{Ee}$. Nonetheless, this scheme is prone to stability problems producing oscillatory problems since the approximation is of order higher than 1.

3.6.3 Quadratic Upwind Interpolation for Convective Kinematics (QUICK)

A logical improvement of CDS is using a parabola to interpolate between nodal points rather than a straight line. To construct a parabola three points are needed. As aforementioned, upstream conditions have a greater influence on flow properties than downstream conditions for incompressible flows and low Mach number gases. QUICK scheme takes profit of this fact. In order to ease the study, some notation is introduced. Located at the face position, D refers to the downstream node, C is the first upstream node and U is the most upstream node.

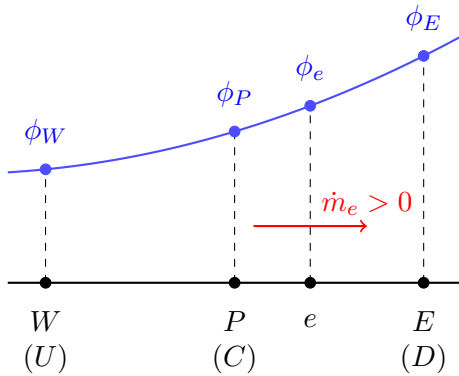


Figure 3.7. QUICK when $(\mathbf{v} \cdot \mathbf{n})_e > 0$.

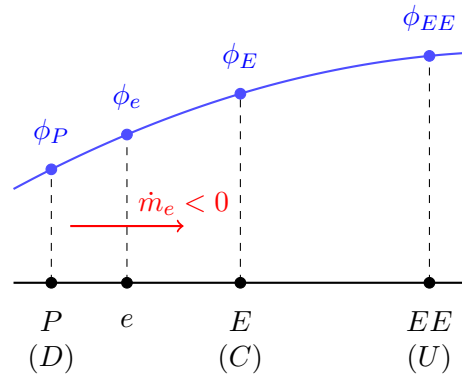


Figure 3.8. QUICK when $(\mathbf{v} \cdot \mathbf{n})_e < 0$.

References

- [1] Suhas V Patankar. *Numerical heat transfer and fluid flow*. McGraw–Hill Book Company, 1980.
- [2] Joel H Ferziger, Milovan Perić, and Robert L Street. *Computational methods for fluid dynamics*. Springer, 2002.